JACS
JOURNAL OF THE AMERICAN CHEMICAL SOCIETY

Article

pubs.acs.org/JACS

Branched Multifunctional Polyether Polyketals: Variation of Ketal Group Structure Enables Unprecedented Control over Polymer Degradation in Solution and within Cells

Rajesh A. Shenoi,[†] Jayaprakash K. Narayanannair,[‡] Jasmine L. Hamilton,[†] Benjamin F. L. Lai,[†] Sonja Horte,[†] Rajesh K. Kainthan,[‡] Jos P. Varghese,[§] Kallanthottathil G. Rajeev,[‡] Muthiah Manoharan,[‡] and Jayachandran N. Kizhakkedathu*[,†,⊥]

[†]Centre for Blood Research and Department of Pathology and Laboratory Medicine, University of British Columbia, Vancouver, British Columbia, Canada V6T 1Z3

[‡]Alnylam Pharmaceuticals, 300 Third Street, Cambridge, Massachusetts 02142, United States

[§]Sanmar Speciality Chemicals Ltd., Chennai, Tamil Nadu, India

[⊥]Department of Chemistry, University of British Columbia, Vancouver, British Columbia, Canada V6T 1Z3

Supporting Information

ABSTRACT: Multifunctional biocompatible and biodegradable nanomaterials incorporating specific degradable linkages that respond to various stimuli and with defined degradation profiles are critical to the advancement of targeted nanomedicine. Herein we report, for the first time, a new class of multifunctional dendritic polyether polyketals containing different ketal linkages in their backbone that exhibit unprecedented control over degradation in solution and within the cells. High-molecular-weight and highly compact poly(ketal hydroxyethers) (PKHEs) were synthesized from newly designed α-epoxy-ω-hydroxyl-functionalized AB_2-type ketal monomers carrying structurally different ketal groups (both cyclic and acyclic) with good control over polymer properties by anionic ring-opening multibranching polymerization. Polymer functionalization with multiple azide and amine groups was achieved without degradation of the ketal group. The polymer degradation was controlled primarily by the differences in the structure and torsional strain of the substituted ketal groups in the main chain, while for polymers with linear (acyclic) ketal groups, the hydrophobicity of the polymer may play an additional role. This was supported by the log *P* values of the monomers and the hydrophobicity of the polymers determined by fluorescence spectroscopy using pyrene as the probe. A range of hydrolysis half-lives of the polymers at mild acidic pH values was achieved, from a few minutes to a few hundred days, directly correlating with the differences in ketal group structures. Confocal microscopy analyses demonstrated similar degradation profiles for PKHEs within live cells, as seen in solution and the delivery of fluorescent marker to the cytosol. The cell viability measured by MTS assay and blood compatibility determined by complement activation, platelet activation, and coagulation assays demonstrate that PKHEs and their degradation products are highly biocompatible. Taken together, these data demonstrate the utility this new class of biodegradable polymer as a highly promising candidate in the development of multifunctional nanomedicine.

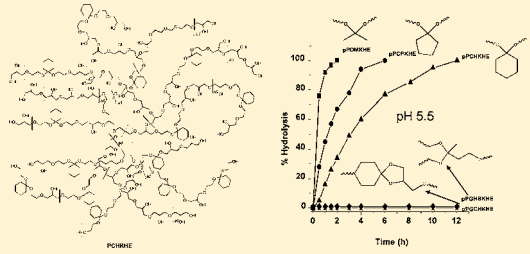

1. INTRODUCTION

The availability of multifunctional biodegradable polymers with defined structure, controlled degradation profiles, and biocompatibility is critical to the development of novel targeted intercellular drug delivery systems, imaging agents, and scaffolds for tissue engineering.[1−3] Structurally different biodegradable polymers with characteristic features such as polyesters, polyorthoesters, polyanhydrides, polyurethanes, polyketals, polyacetals, and disulfide-containing polymers undergo degradation to various extents *in vitro* and/or *in vivo* via hydrolysis, enzymatic degradation, pH changes, and redox reactions.[4−15] The presence of multiple reactive functionalities on the polymer along with defined biodegradation profiles, water solubility, and biocompatibility are critical for developing targeted drug delivery devices. pH-degradable polymers are of special interest due to their broad range of applications such as tumor targeting, delivery of protein-based vaccines, nucleic acid delivery, and treatment of acute inflammatory diseases.[16] The acidic nature of tumor tissues necessitates the need for pH-responsive/degradable formulations for enhanced tumor targeted therapy, while protein and nucleic acid delivery requires the rapid endosomal degradation of the polymeric carrier to generate osmotic imbalance and release of the payload into the cytosol.[17]

Received: May 25, 2012
Published: August 20, 2012

 © 2012 American Chemical Society dx.doi.org/10.1021/ja305080f | *J. Am. Chem. Soc.* 2012, 134, 14945−14957

Table 1. Structure and Characteristics of Synthesized α-Epoxy-ω-hydroxyl Ketal Monomers

Monomer name	Chemical structure	Log P[a]	$t_{1/2}$ hydrolysis at pH 5.5 (min)
2-{1-methyl-1-[2-(oxiran-2-yl methoxy) ethoxy] ethoxy} ethanol **(DMKM)**	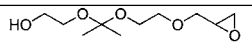	-0.94	6.3
2-(1-(2-(oxiran-2-ylmethoxy) ethoxy) cyclohexyloxy) ethanol **(CHKM)**	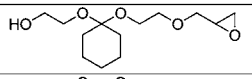	0.46	19.8
2-[1-(2-oxiranylmethoxy-ethoxy)-cyclopentyloxy]-ethanol **(CPKM)**	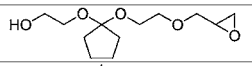	0	11
2-(2-methyl-4-((oxiran-2-yl methoxy)methyl)-1,3-dioxolan-2-yl)ethanol **(GHBKM)**	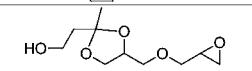	-0.79	Very slow hydrolysis
(8-(oxiran-2-ylmethoxy)-1,4-dioxaspiro [4.5] decan-2-yl) methanol **(GCHKM)**	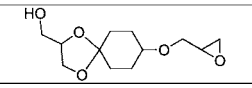	-0.39	Very slow hydrolysis

[a]Calculated using ALOGP program as per ref 29.

A

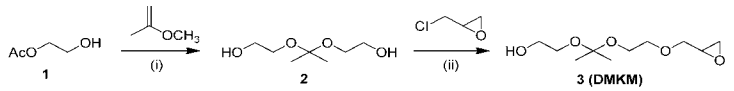

i) a. PPTS, THF, molecular sieve 5Å, rt, 48 h, 60%; b) K_2CO_3, MeOH, rt, 92%; (ii) Na, *i*PrOH, 15 h, rt, 40%

B

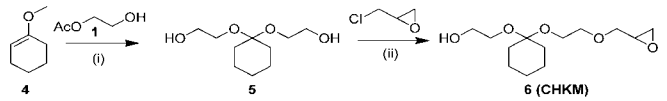

(i) a. PTSA, molecular sieve 5Å, THF, 46%; b) K_2CO_3, MeOH, 94%. (ii) Potassium-*t*-butoxide, *t*-Butanol, rt, 40%.

C

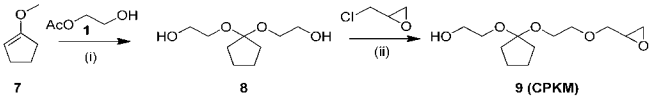

(i) a. PPTS, THF, 50%; b) K_2CO_3, MeOH, 50%. (ii) Potassium-*t*-butoxide, THF, rt, 30%.

D

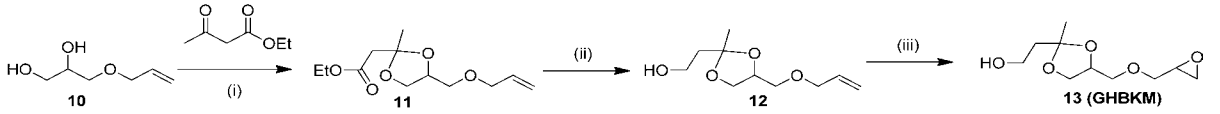

(i) PTSA, EDC, reflux, 73%; (ii) $LiAlH_4$, THF, 94%; (iii) MCPBA, DCM , rt, 68%

E

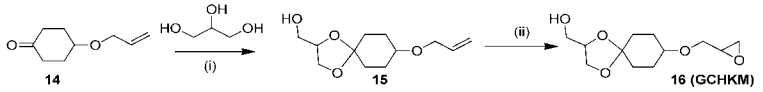

(i) PTSA, THF, molecular sieve MS, 15 h, rt, 85%; (ii) MCPBA, DCM, rt, 50%.

Figure 1. Synthetic schemes for different α-epoxy-ω-hydroxyl ketal monomers.

Among the pH-degradable polymeric systems, polyketals are of particular interest as they are neutral and generate nontoxic neutral degradation products. Polymers with a main-chain degradable dimethyl ketal group have been reported as delivery vehicles for therapeutic agents.[18−20] Murthy and co-workers reported poly(1,4-phenyleneacetone dimethylene ketal) and poly(cyclohexane-1,4-diyl acetone dimethylene ketal), both containing a dimethyl ketal group, as a new class of pH-sensitive drug delivery vehicle.[18] Dimethyl ketal group-containing polyurethane and linear poly(amido amines) have been studied by the group of Frechet for applications such as drug delivery and protein-based vaccines.[19a,b] Frechet's group also reported the enhanced cellular uptake of microparticles based on a copolymer of a dimethyl ketal group containing cross-linker with a cell-penetrating peptide containing acryl-amide.[19c] Microparticles based on acetalated dextran containing both linear and cyclic dimethyl ketal groups have been explored as drug delivery vehicles for immunotherapy.[19d] There has been a recent report on poly(β-amino ester ketal) nanoparticles that contain both a β-amino ester and dimethyl ketal group in the backbone as a dual pH-sensitive drug delivery vehicle.[20] However, all these polyketal polymers are linear, have same degradable dimethyl ketal linkages, have low molecular weights, and lack the multifunctionality and water solubility desired for several applications.[21] Moreover, in most of the cases the hydrolysis half-lives of these polymers were changed by altering

dx.doi.org/10.1021/ja305080f | J. Am. Chem. Soc. 2012, 134, 14945−14957

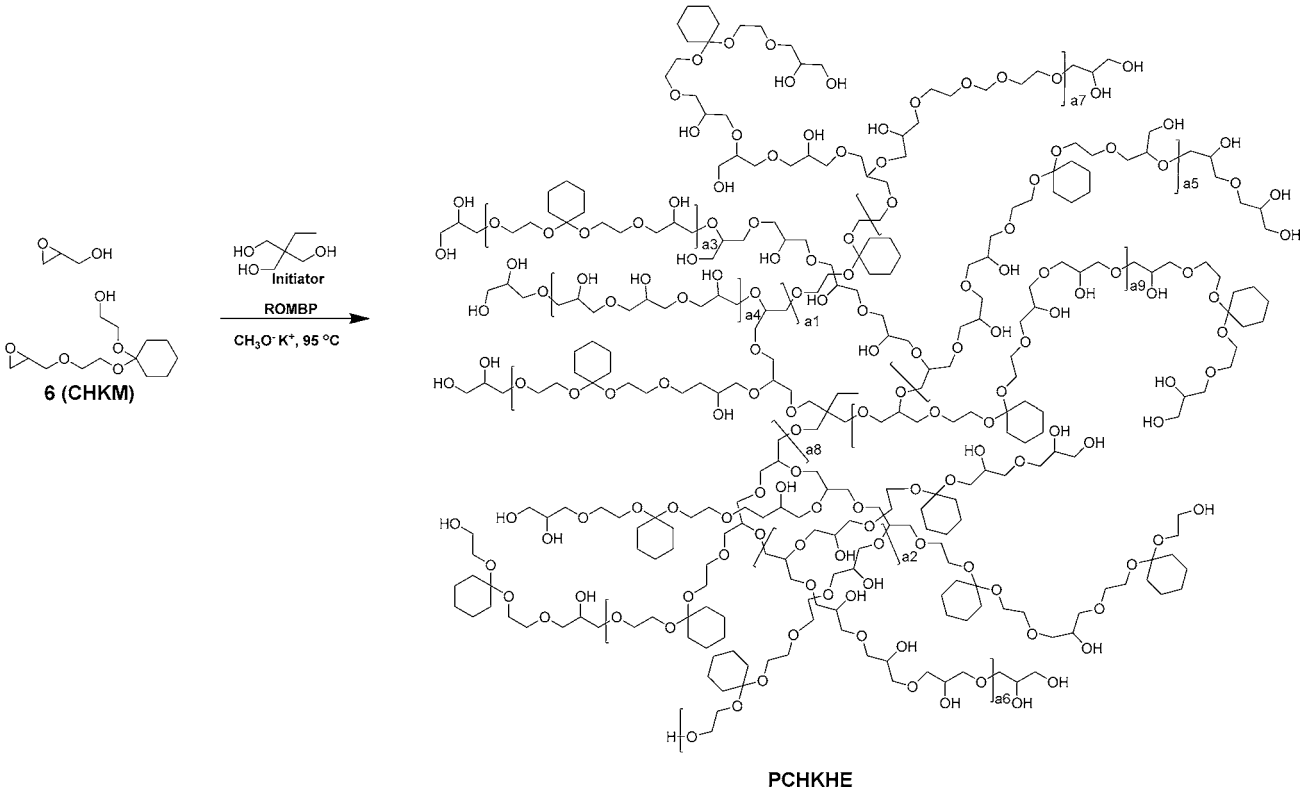

Figure 2. General scheme for the synthesis of poly(ketal hydroxyethers). Scheme for the synthesis of copolymer of 2-(1-(2-(oxiran-2-ylmethoxy)ethoxy)cyclohexyloxy)ethanol and glycidol by anionic multibranching ring-opening polymerization is shown. Other PKHEs were synthesized by a similar method.

the diffusion of water to predominantly hydrophobic polymers, which is very difficult to control. The hydrolysis rate also depended on the physical nature of the polymeric systems; for instance, nanoparticles degrade much rapidly than microparticles or a film of the polymer. The degradation rate also depended on various processing conditions used.[18−20] This limitation is in fact true for many of other types of biodegradable polymeric systems currently available and is a major obstacle for their use in the enhanced delivery of bioactive molecules within the cells.[8,22] Hence there is a need for developing new biocompatible biodegradable polymers that possess the features of high pH sensitivity, multifunctionality, increased/enhanced water solubility, and defined degradation profiles for improved targeted drug delivery and enhanced rapid endosomal escape/release of bioactive molecules.

Herein we report, for the first time, the design, synthesis, pH-dependent degradation, and biocompatibility studies of a novel class of well-defined branched multifunctional polyether polyketals, poly(ketal hydroxyethers) (PKHEs), by anionic ring-opening multibranching polymerization (ROMBP) of newly developed functional AB_2-type ketal monomers. The PKHEs incorporate features such as high molecular weight, water solubility, multifunctionality, excellent biocompatibility, and defined pH-dependent degradability both in buffer solutions and within the cells. We also demonstrate for the first time that the biodegradability of the polyketals can be controlled by incorporating structurally different ketal linkages in their backbone, and PKHE polymers degrade with unprecedented control to low-molecular-weight, neutral, nontoxic, and easily excretable products. Our data demonstrate that the new PKHE polymers have considerable potential in the development of multifunctional drug delivery devices for efficient endosomal escape and cytosolic delivery.

2. RESULTS AND DISCUSSION

2.1. Development of α-Epoxy-ω-hydroxyl-Functionalized AB_2-Type Ketal Monomers. To achieve controlled pH degradability and multifunctionality of polymers, we first designed and synthesized five novel heterofunctional AB_2-type monomers with structurally different ketal groups (Table 1) that can be polymerized by ROMBP. These monomers are DMKM (**3**), CHKM (**6**), CPKM (**9**), GHBKM (**13**), and GCHKM (**16**), each containing an epoxide group, a hydroxyl group, and a different type of ketal group per molecule.

New synthetic schemes were developed for the monomers as shown in Figure 1. Monomers with linear (acyclic) ketal groups (**3**, **6**, **9**) were synthesized starting from ethylene glycol. As shown in Figure 1A, the monomer DMKM was synthesized from ethylene glycol monoacetate (**1**),[23] which was reacted with 2-methoxypropene in the presence of *p*-toluenesulfonic acid (PTSA) to obtain the corresponding dimethyl ketal diacetate intermediate. The compound was then deacetylated using potassium carbonate in methanol to obtain the dimethyl ketal diol **2**. Reaction of the ketalized diol with sodium/isopropanol followed by reaction with epichlorohydrin afforded the DMKM monomer **3**. Synthesis of CHKM monomer (Figure 1B) was started from the cyclohexanone enol ether (**4**).[24] Reaction of ethylene glycol monoacetate with **4** in the presence of PTSA in anhydrous THF gave the corresponding ketalized diacetate intermediate. Deprotection of acetyl group from the diacetate with potassium carbonate in methanol yielded the ketalized diol **5**. Treatment of the diol **5** with

dx.doi.org/10.1021/ja305080f | J. Am. Chem. Soc. 2012, 134, 14945−14957

Table 2. Characteristics of Poly(ketal hydroxyethers) Synthesized by ROMBP

PKHE	feed ratio TMP:ketal:glycidol (mmol)[a]	conv (%)	M_n (M_w/M_n)[b]	R_h (nm)[c]	polymer composition ketal:glycidol[d]
PDMKHE-1	0.357:7.73:2.61	64	8500 (1.6)	2.8	52:48
PDMKHE-2	0.357:15.91:5.38	60	18900 (1.48)	3.3	56:44
PDMKHE-3	0.357:31.8:10.8	70	28200 (1.44)	3.2	66:34
PCHKHE-1	0.357:13:4.2	54	8300 (1.41)	3.4	54:46
PCHKHE-2	0.357:19.2:6.1	63	18300 (1.44)	3.8	53:47
PCHKHE-3	0.268:22:7.2	62	22000 (1.34)	4.2	60:40
PCHKHE-4	0.224:30.8:10.5	55	56700 (1.6)	5.2	65:35
PCPKHE-1	0.357:7.32:2.4	45	6200 (1.7)	2.6	52:48
PCPKHE-2	0.357:32.5:11	60	14000 (1.65)	3.5	62:38
PGHBKHE-1	0.357:32.1:10.8	62	7000 (1.6)	3.2	57:43
PGCHKHE-1	0.357:28.7:9.6	60	8600 (1.58)	3.3	55:45

[a]For all experiments, temperature was 95 °C and polymerization time was 24 h. [b]Determined by GPC-MALLS analysis in chloroform. [c]Determined by QELLS analysis in chloroform. [d]Calculated from ^{1}H NMR spectra; feed composition of ketal:glycidol was 75:25 for all experiments.

epichlorohydrin in the presence of potassium *tert*-butoxide in *tert*-butanol afforded the epoxide-functionalized cylcohexyl ketal monomer **6** (CHKM). The CPKM monomer **9** was synthesized from cyclopentanone enol ether using a procedure similar to that used for CHKM (Figure 1C).

The monomers GHBKM and GCHKM were synthesized from glycerol as the starting material. For the synthesis of GHBKM (Figure 1D), glycerol was first converted into its α-monoallyl ether **10**.[25] Reaction of **10** with ethyl acetoacetate in the presence of PTSA in anhydrous ethylene dichloride yielded ketal derivative **11**, and subsequent reduction of the ester group using lithium aluminum hydride in anhydrous THF yielded the alcohol **12**. In the final step, epoxidation of the double bond was achieved by reacting with *m*-chloroperbenzoic acid in dichloromethane to afford the GHBKM monomer **13**. Similarly, GCHKM monomer was synthesized by the reaction of glycerol with 4-(2-propenyloxy)cyclohexanone (**14**).[26] Ketalization followed by epoxidation of the double bond afforded the required GCHKM monomer **16** as shown in Figure 1E. All monomers were purified by column chromatography and characterized by NMR and high-resolution mass spectrometric analyses (Figures S1−S10, Supporting Information).

2.2. Synthesis of PKHEs by Anionic ROMBP. After synthesis of AB_2-type monomers, we explored their anionic ROMBP using trimethylol propane/potassium methoxide as the initiator system at 95 °C. A representative synthetic scheme for the polymerization of CHKM is shown in Figure 2. Homopolymerization of the ketal monomers resulted in low conversions (∼15−20%); however, the addition of glycidol as a comonomer significantly improved the monomer conversions. Thus, employing an initial feed ratio of ketal monomer to glycidol in the molar composition 3:1 (Table 2), poly(dimethylketal hydroxyether) (PDMKHE), poly(cyclopentylketal hydroxyether) (PCPKHE), poly(cyclohexylketal hydroxyether) (PCHKHE), poly(glycerol hydroxybutanone ketal hydroxyether) (PGHBKHE), and poly(glycerol cyclohexanone ketal hydroxyether) (PGCHKHE) having 52−66 mol % incorporation of ketal groups in the polymer backbone were synthesized (Table 2). Polymers of different molecular weights (6−57 kg/mol) and relatively low molecular weight distributions were synthesized by varying the monomer-to-initiator molar ratio. The polydispersity index of the PKHE polymers was consistent with the reported values for the multibranching polymerization of AB_2-type monomers.[27] The incorporation of ketal monomers was lower than the initial feed composition, suggesting that ketal monomers were less reactive than glycidol. The structure of the ketal group was also found to have an effect on the reactivity of the monomers toward ROMBP, as evident from the differences in the copolymer compositions compared to initial feed ratio as well as the relatively low conversion for certain monomers (Table 2). The monomers containing acyclic ketal groups (DMKM, CPKM, and CHKM) were found to be slightly more reactive than monomers containing cyclic ketal structures (GHBKM and GCHKM). Also, at similar monomer-to-initiator ratios, GHBKM and GCHKM gave lower molecular weights compared to other monomers.

All the PKHEs were soluble in organic solvents such as methanol, chloroform, THF, and DMF; however, only poly(dimethylketal hydroxyether) (PDMKHE) was soluble in water. The GPC chromatograms of PKHE polymers showed monomodal distribution of molecular weights (Figure S11). ^{1}H NMR spectra of the polymers showed characteristic peaks due to the presence of ketal groups in the polymer (Figures S12−S14). PDMKHE gave a signal at 1.25 ppm that corresponds to the methyl resonance of the dimethyl ketal group. For PCPKHE and PCHKHE, signals due to the methylene resonance of the cyclopentyl and cyclohexyl ketal groups respectively were observed in the region 1.3−1.8 ppm. Signals at 1.2−1.3 ppm were found for PGHBKHE that correspond to the methyl groups of the hydroxybutanone ketal group. NMR spectra of the polymers together with the molecular weight analysis in chloroform confirmed the formation of high-molecular-weight multifunctional polymeric structure with intact ketal moieties. A peak corresponding to −OH stretching around 3300 cm^{-1} in the FTIR spectra of the PKHE polymers and a characteristic signal between 4.5 and 4.8 ppm in the NMR spectra of polymers in DMSO-d_6 confirmed the presence of hydroxyl groups in the polymers (Figures S12−S15).

The branched structure of the PKHE polymers was probed by inverse-gated ^{13}C NMR analysis. A representative NMR spectrum for PDMKHE is shown in Figure S16. The signals at 25.37 and 101.33 ppm confirmed the presence of dimethyl ketal groups in the polymer. The polymer has linear, dendritic, and terminal structural units that are usually observed with other hyperbranched polymers.[28] The degree of branching calculated from the spectra was in the range 0.50−0.60 for different PKHE polymers and is very close to the values reported for hyperbranched polymers obtained from AB_2-type monomers.[28] The ^{13}C NMR spectra also revealed that the ketal groups were randomly distributed throughout the polymer. The

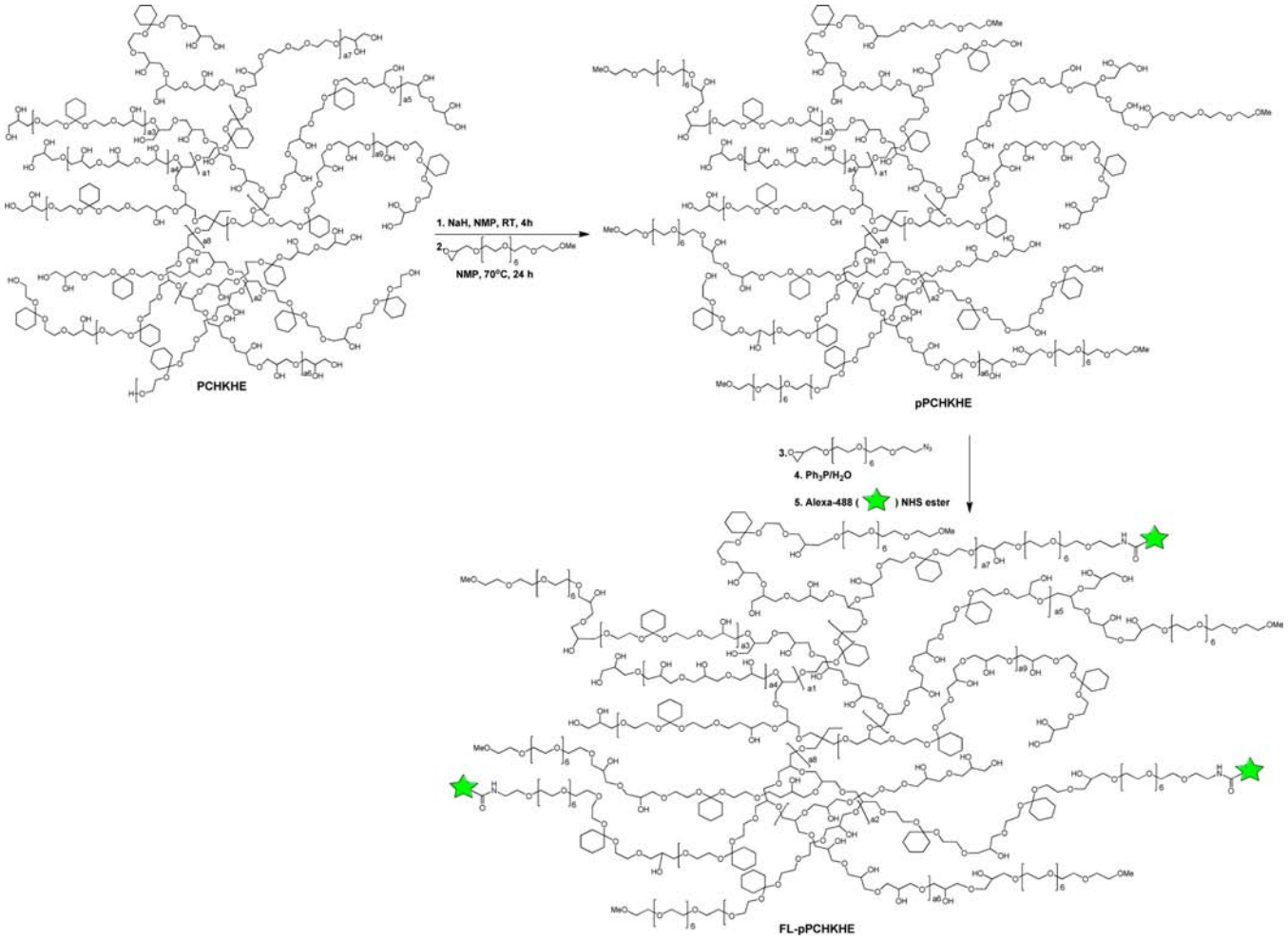

Figure 3. Polymer modification and functionalization: scheme for PEG modification, azide and amine functionalization, and development of fluorescently labeled polymers. Shown is an example for PCHKHE polymer functionalization. Other PKHE polymers were modified by similar methods.

Table 3. Characteristics of pPKHEs and Their pH-Dependent Hydrolysis in Various Buffer Solutions

				hydrolysis half-life (h)							
				pH 5.5		pH 6.0		pH 6.5		pH 7.4	
polymer	mPEG content (mol %)	M_n (M_w/M_n)[a]	R_h[b] (nm)	25 °C	37 °C	25 °C	37 °C	25 °C	37 °C	25 °C	37 °C
pPDMKHE-3	28	38000 (1.3)	5.4	0.3	very fast[c]	1.1	0.16	3.5	0.43	21.6	3.9
pPCPKHE-2	30	29000 (1.7)	3.3	0.8	0.18	2.2	0.5	6.9	1.4	69.3	17.3
pPCHKHE-3	30	37800 (1.5)	4.5	2.5	0.82	8.7	2.5	15.9	9.0	187	79
pPGHBKHE-1	25	13800 (1.4)	3.8	25300	3650	nd[d]	nd	nd	nd	very slow[e]	very slow[f]
pPGCHKHE-1	30	22000 (1.8)	4.2	21120	2950	nd	nd	nd	nd	very slow[e]	very slow[f]

[a]Determined by GPC-MALLS in 0.1 M $NaNO_3$ at pH 8.5. [b]Determined by QELLS in 0.1 M $NaNO_3$ at pH 8.5. [c]Hydrolysis was 100% at the first time point of NMR analysis (30 min). [d]nd = not determined. [e]No measurable hydrolysis observed in 400 days. [f]5% hydrolysis observed in 400 days.

spectra showed characteristic signals for the presence of linear (L), dendritic (D), and terminal (T) units for hyperbranched structures. Since the terminal structural units (signal at 64−65 ppm) come primarily from glycidol component of the copolymer, the NMR data support the random distribution of ketal groups within the polymer. Evidence for the compact nature of the polymers was also obtained from their relatively small hydrodynamic radii (2.6−5.2 nm, Table 2) measured by dynamic light scattering.

2.3. Effect of Ketal Structure on Polymer Degradation in Aqueous Buffer solutions. The presence of ketal groups in the monomers and the polymers makes them susceptible to cleavage under acidic conditions. In order to compare the degradation of the polymers in aqueous buffer conditions, it is necessary that all the polymers have similar water solubility. To achieve this, a portion of the hydroxyl groups of PKHEs was deprotonated with sodium hydride followed by reaction with α-methoxy-ω-epoxy polyethylene glycol ($mPEG_{400}$-epoxide) to generate PEGylated PKHEs (pPKHEs) (Figure 3). The polymers PDMKHE-3, PCHKHE-3, PCPKHE-2, PGHBKHE-1, and PGCHKHE-1 were selected for modification using $mPEG_{400}$-epoxide. Detailed characteristics of the modified

dx.doi.org/10.1021/ja305080f | J. Am. Chem. Soc. 2012, 134, 14945−14957

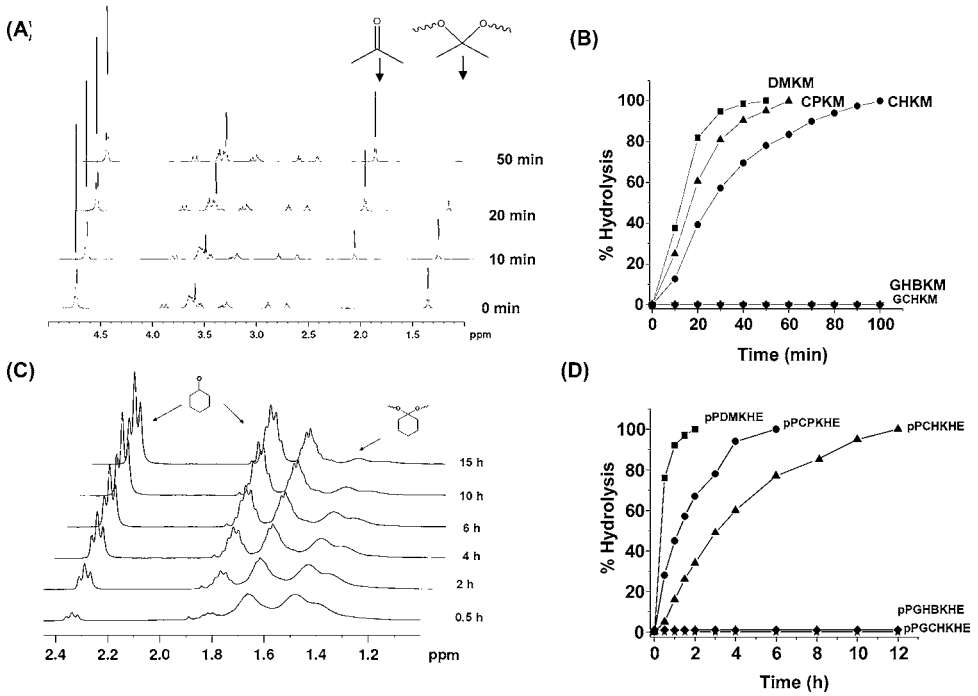

Figure 4. Comparison of degradation of ketal monomers and polymers in aqueous phosphate buffer at pH 5.5 in D_2O at 25 °C. (A) ^1H NMR spectra showing the hydrolysis of DMKM. (B) Comparison of hydrolysis kinetics plots of various ketal monomers. The percentage of hydrolysis is calculated from the ^1H NMR integration data. (C) ^1H NMR spectra showing the degradation of pPCHKHE-3. (D) Comparison of hydrolysis kinetics plots of different pPKHEs. The percentage of hydrolysis was calculated from the ^1H NMR integration data.

PKHEs are given in Table 3. The polymers have 25−30 mol % of mPEG and were found to be highly water-soluble. The presence of mPEG in the polymers was confirmed by ^1H NMR analysis and also from the increase in the absolute molecular weights of the modified PKHEs compared to the original polymers (Tables 2 and 3). For example, the M_n of PDMKHE-3 was increased from 28 200 to 38 000 g/mol upon incorporation of ∼28 mol % of mPEG chains. The ketal groups were stable during the modification as evident from NMR and molecular weight analyses. The very small hydrodynamic radii (3.3−5.4 nm) of pPKHEs (Table 3) along with high branching density confirm the highly compact structure of these polymers in water without aggregation. The water solubility, compact structure, polyether backbone, and multifunctionality differentiate the current class of ketal polymers from previously reported polyketal polymers.[18−20]

2.3.1. Degradation of α-Epoxy-ω-hydroxyl Ketal Monomers at pH 5.5. Initially, the degradation kinetics of the monomers was studied by dissolving them in phosphate buffer at pH 5.5 prepared in D_2O and recording the ^1H NMR spectra at 25 °C at different time intervals. The percent of hydrolysis was calculated from the disappearance of signals corresponding to the ketal functionality and the simultaneous appearance of signals due to the formation of the corresponding ketone. Thus, for the monomer DMKM, the peak at 1.39 ppm due to the dimethyl ketal moiety gradually disappeared and a new peak appeared at 2.19 ppm due to the formation of acetone (Figure 4A). Similarly other monomers also exhibited characteristic signals for the ketal and ketone moieties. The new monomers exhibited ketal group structure-dependent hydrolysis; the monomers with acyclic ketal structure (DMKM, CPKM, and CHKM) were hydrolyzed much faster compared to those with cyclic structure (GHBKM and GCHKM) (Figure 4B). The hydrolysis half-lives ($t_{1/2}$) at pH 5.5 were 6.3, 11, and 19.8 min respectively for the monomers DMKM, CPKM and CHKM, while GHBKM and GCHKM were not hydrolyzed for several days at this pH (Table 1).

2.3.2. Degradation of Modified pPKHEs at pH 5.5. We then studied the hydrolysis of the pPKHEs at pH 5.5 in a similar manner to that of the monomers by monitoring the decrease in the intensity of the signals due to the ketal groups and corresponding appearance of ketone group. Representative NMR spectra showing degradation profiles of pPCHKHE-3 is shown in Figure 4C. The cyclohexyl group of the ketal moiety in pPCHKHE-3 polymer had a broad characteristic signal between δ 1.39 and 1.75 ppm. Upon degradation, the intensity of this peak gradually decreased, and new sharp characteristic NMR signals appeared at δ 1.85 and 2.34 ppm due to formation of cyclohexanone (Figure 4C). The percentage of degradation was calculated from the ratio of the intensities of the NMR signals corresponding to the cyclohexyl ketal group within the main chain and the cyclohexanone. Similar observations were seen for other pPKHE polymers (Figures S17−S19). The polymers exhibited a similar trend in the hydrolysis as was observed with the corresponding monomers; however, the hydrolysis rate was slower. The hydrolysis rate followed the order pPDMKHE-3 > pPCPKHE-2 > pPCHKHE-3 ≫ pPGHBKHE-1 ≈ pPGCHKHE-1 (Figure 4D). As shown in Table 3, the hydrolysis half-lives at pH 5.5 for pPDMKHE-3, pPCPKHE-2, pPCHKHE-3, pPGHBKHE-1, and pPGCHKHE-1 were 0.3, 0.8, 2.5, 25 300, and 21 120 h, respectively. In contrast to pPDMKHE-3, pPCPKHE-2, and pPCHKHE-3 with acyclic ketal structures, the polymers containing cyclic 1,3-dioxolane (pPGHBKHE-1) and spiro ketal groups (pPGCHKHE-1) were more stable towards hydrolysis.

The observed differences in the hydrolysis rates of the monomers and polymers may be attributed to several factors:

dx.doi.org/10.1021/ja305080f | J. Am. Chem. Soc. 2012, 134, 14945−14957

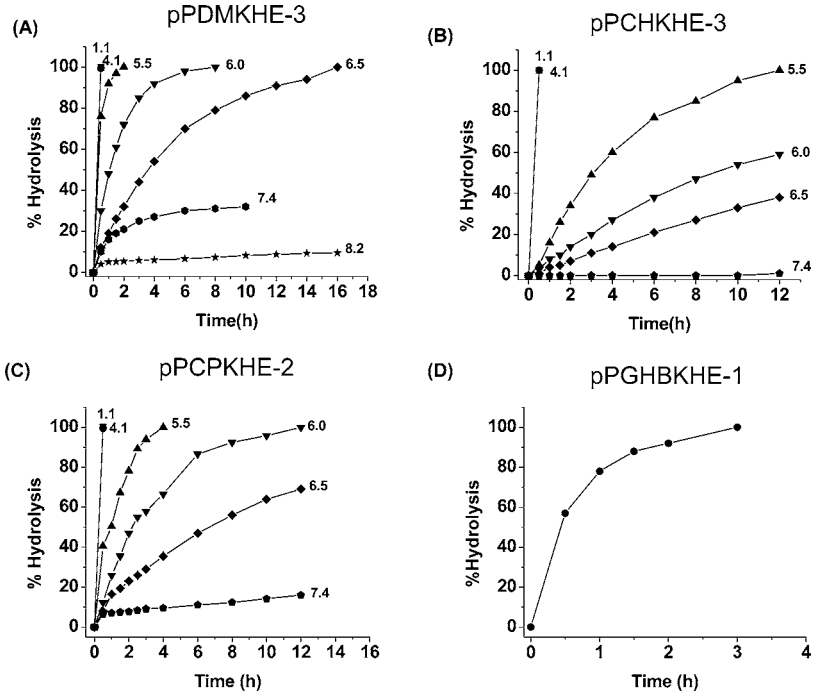

Figure 5. Comparison of pH-dependent degradation of pPKHEs at 25 °C at different pH values in aqueous buffer solutions measured by NMR analysis. pH-dependent degradation of (A) pPDMKHE-3, (B) pPCHKHE-3, and (C) pPCPKHE-2. (D) Degradation of pPGHBKHE-1 at pH 1.1. The pH values of the solutions are shown in the graph.

(i) the differences in hydrophobicity of the groups surrounding the ketal moiety, (ii) the ring strain of cyclic ketal groups, and (iii) the differences in the ketal structure. All these factors can alter their reactivity toward acids during hydrolysis.

In order to verify whether the observed differences in the hydrolysis rate of the monomers is due to the differences in hydrophobic character of the monomers, we calculated the log *P* value (which is a measure of the hydrophobicity of the molecule) using the ALOGP program.[29] The total number of carbon atoms in the current monomer set ranged from 10 to 13, and all the monomers had the same number of oxygen atoms per molecule (Table 1). The CHKM monomer had the highest number of carbon atoms per molecule among the monomers. The calculated log *P* values were −0.94, 0.0, 0.46, −0.79, and −0.39 for monomers DMKM, CPKM, CHKM, GHBKM, and GCHKM, respectively, which suggest that their hydrophobicity was in the order CHKM > CPKM > GCHKM > GHBKM > DMKM (Table 1). The degradation of the monomers followed the order DMKM > CPKM > CHKM ≫ GHBKM ≈ GCHKM (Figure 4B), which suggests that the hydrophobicity of monomers may not be influencing the degradation.

Although we anticipated similar hydrophobicity for the polymers prepared from these monomers, we investigated the hydrophobic character of the modified polymers by fluorescence spectroscopy using pyrene as the probe. The vibrational spectrum of pyrene is known to be sensitive to the hydrophobicity of its environment and can be measured from the ratio of the intensities of the first (I_1 = 372 nm) and third (I_3 = 384 nm) peaks in the fluorescence spectrum.[30a] For instance in aqueous solutions, the I_1/I_3 values will be in the range 1.9−2.0, and in the hydrophobic nonpolar environments, they will be 0.55−0.6.[30a] Kalyanasundaram et al. also reported that for micellar systems the I_1/I_3 value ranges from 1 to 1.4, depending on the nature of the micelle.[30a] For PS-PEG block copolymers, the I_1/I_3 value reported was between 1.1 and 1.2 in aqueous conditions.[30c] Pyrene fluorescence spectra in the presence of PEGylated PKHEs at two different concentrations (0.4 and 4 mg/mL) were obtained. The I_1/I_3 values for different polymers at 0.4 mg/mL concentration was 1.80, 1.55, 1.64, and 1.74 respectively for pPDMKHE, pPCPKHE, pPCHKHE, and pPGHBKHE (Table S1 and Figure S20) and followed a trend similar to that of the hydrophobicity values calculated from log *P* values for the corresponding monomers. Though the I_1/I_3 values suggest a slightly hydrophobic environment for these polymers, they were higher than the range (1.0−1.4) reported for micellar systems[30a−c] and very close to that reported for PEG (1.58−1.60).[30d] The data suggest that the pPKHEs may have a highly hydrated core−shell structure in water. Since the hydrophobicity values do not correlate with the degradation profile (Figure 4D), we can confirm that, globally, the hydrophobicity differences of the polymers do not have a significant role in controlling the polymer degradation. However, in the case of acyclic ketal polymeric structures (pPDMKHE, pPCPKHE, and pPCHKHE), the hydrophobicity trend measured by pyrene fluorescence followed the same trend as the log *P* values calculated for different monomers. The polymer degradation also followed a similar trend. Thus, the influence of hydrophobicity changes on polymer degradation cannot be completely ruled out for acyclic ketal polymeric structures.

These results are also supported by the literature evidence on small organic molecules containing ketal groups, where it has been shown that the groups attached to the ketal structure can influence the reactivity of ketal groups.[31,32] Significant differences in the hydrolysis rates were observed between diethyl ketals of cyclopentanone and cyclohexanone, with the rate of hydrolysis for cyclopentanone ketal being 3 times faster than that of cyclohexanone ketal.[31] The decrease in the torsional strain energy for the cyclopentanone derivative as a result of the

dx.doi.org/10.1021/ja305080f | J. Am. Chem. Soc. 2012, 134, 14945−14957

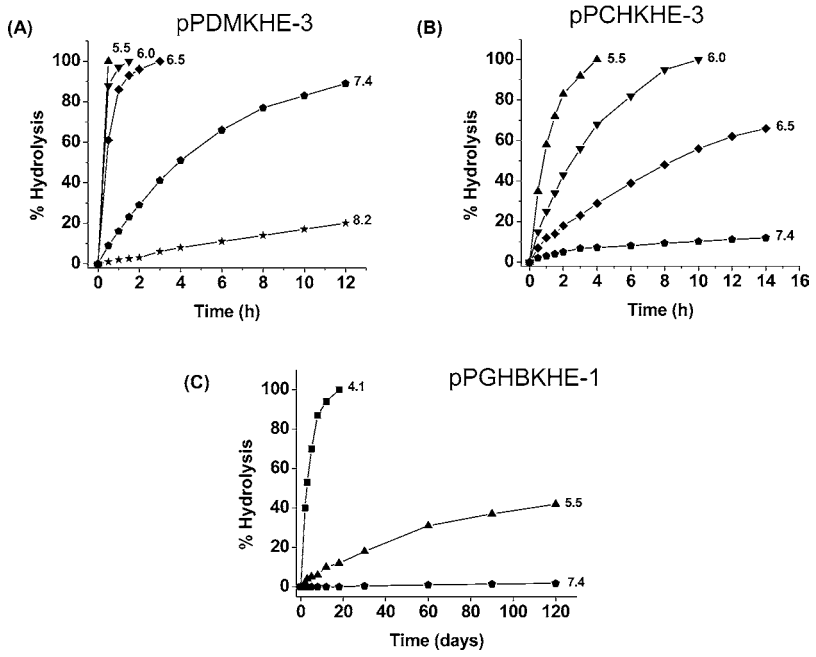

Figure 6. Comparison of pH-dependent degradation of pPKHEs at 37 °C at different pH values in aqueous buffer solutions measured by NMR analysis. pH-dependent degradation of (A) pPDMKHE-3, (B) pPCHKHE-3, and (C) pPGHBKHE-1. The pH values of the solutions are shown in the graph.

activation process involved in hydrolysis was attributed to this observation. It has been also shown that a slight increase in the torsional energy strain for the cyclohexanone ketal results in slower hydrolysis rates.[31] In the case of GHBKM and GCHKM, the ketal group is part of the ring, and cleavage of the ring (endocyclic cleavage) must take place during hydrolysis, which occurs at much slower rates.[32] Based on this evidence from the low-molecular-weight molecules, we attribute the differences in the hydrolysis rates of the PKHE polymers primarily to the differences in the ketal group structure and ring strain of the groups with minor dependence on the polymer hydrophobicity.

In the pyrene fluorescence measurements, slightly lower I_1/I_3 values (1.41−1.55) were obtained at higher polymer concentration (4 mg/mL) compared to 0.4 mg/mL (Table S1). These data suggest that a slightly more hydrophobic environment for pyrene exists at higher polymer concentrations. To investigate whether such differences influence pPKHE degradation, we studied the degradation at two different polymer concentrations, 4 and 20 mg/mL. Our results (Figure S21) showed that polymer degradation was independent of polymer concentration. These data also support the insignificant role of hydrophobicity in polymer degradation.

It is also important to understand if there is any broadening or attenuation of the signals in the NMR spectrum of the polymers due to the formation of unimolecular micelles, as the pPKHEs have a hydrated core−shell structure. This may affect the accuracy of the degradation kinetics since the polymer degradation was measured from the integration of the peaks of the polymer and the ketones resulting from degradation. To probe this, initially the NMR spectra of pPKHEs were recorded in D_2O and $CDCl_3$. In both solvents, the ratio of the intensities of peaks from polyether backbone and PEG chains to ketal groups remained similar (Figures S22−S24), which suggests that solvents did not have any effect on the NMR peak intensity. If there was any attenuation of the signals due to the micelle formation in water, quite different behavior would have been observed, as these polymers were not expected to adopt a micellar structure in chloroform. Moreover, the ratio of the total intensity of the signals from the ketal and ketone groups to that of the polyether backbone and PEG chains remained constant throughout the degradation. In the case of the polymers pPGHBKHE-1 and pPGCHKHE-1, the ketone structure remains as part of the degraded polymer, and no small molecule was formed in this case. Taken together with polymer degradation studied at different polymer concentrations (Figure S21), these data support the fact that the degradation rate of the polymers could be accurately measured from the signals corresponding to the ketal and ketone groups in the NMR spectra. Similar methods have been reported by Broaders et al. previously.[19d]

2.3.3. Effect of pH on the Degradation of pPKHEs. We further investigated the degradation kinetics of pPKHE polymers at different pH values (1.1−8.2) at 25 °C. The hydrolysis profiles for the polymers shown in Figure 5 demonstrate that pPDMKHE-3, pPCHKHE-3, and pPCPKHE-2 with linear (acyclic) ketal groups were completely hydrolyzed at pH 1.1 and 4.1 within a few minutes (Figure 5A−C). A more controlled degradation was observed in the pH range 5.5−8.2, with the hydrolysis rates being slower at higher pH values. For instance, the hydrolysis half-lives ($t_{1/2}$) for pPCHKHE-3 were 2.5, 8.7, 15.9, and 187 h at pH 5.5, 6.0, 6.5, and 7.4, respectively (Table 3), and the polymer was relatively stable at physiological pH and above. A similar trend was observed for the hydrolysis of polymers containing dimethyl and cyclopentyl ketal groups (Figure 5A,C, Table 3). The hydrolysis of pPGHBKHE-1 and pPGCHKHE-1 were much slower even at acidic pH values (Figure 5D). While the polymers with linear ketal groups were hydrolyzed within a few minutes at pH 1.1 and 4.1, the hydrolysis half-life of pGHBKHE-1 at these pH values at 25 °C was 0.5 and 1400 h, respectively. Both pPGHBKHE-1 and pPGCHKHE-1 were very stable at pH above 5.5; pPGHBKHE-1 showed only 30%

dx.doi.org/10.1021/ja305080f | J. Am. Chem. Soc. 2012, 134, 14945−14957

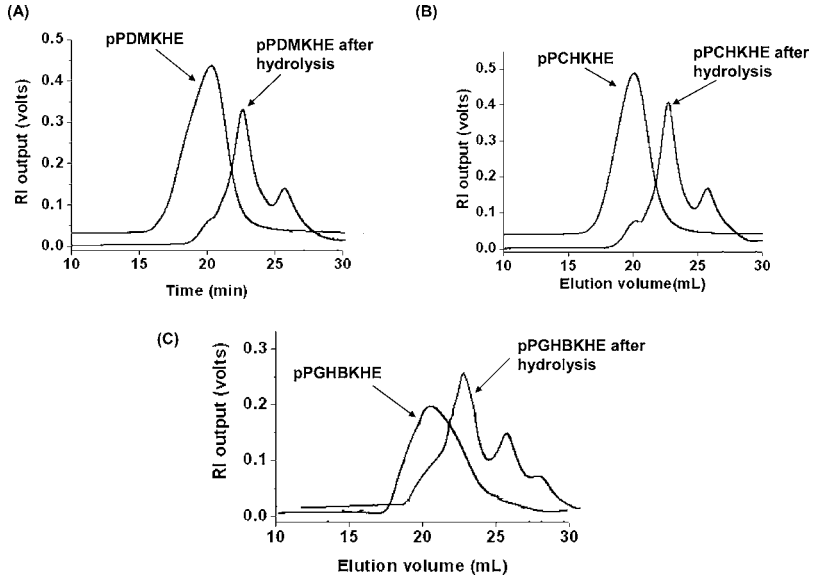

Figure 7. Polymer degradation studied by GPC analysis. PKHE polymers were degraded in 0.1 N HCl, neutralized, and analyzed. GPC chromatograms of pPKHEs before and after the degradation are shown for (A) pPDMKHE-3, (B) pPCHKHE-3, and (C) pPGHBKHE-1.

degradation in 400 days at pH 5.5 and 25 °C. Thus we have shown that a range of hydrolysis half-lives can be achieved by changing the bonding structure of the ketal groups in the polymer backbone and the pH of the solution.

2.3.4. Effect of Temperature on the Degradation of pPKHEs. In order to simulate the hydrolysis behavior of the polymers under physiological conditions and within cells, the polymer degradation was studied at 37 °C. A 3- to 4-fold increase in hydrolysis rates was observed at 37 °C compared to those at 25 °C for a given pH (Figure 6 and Table 3). For example, the $t_{1/2}$ of pPDMKHE-3 at pH 6.0 decreased from 1.1 to 0.16 h when the temperature was increased from 25 °C to 37 °C (Figure 6A, Table 3). Similarly, pPCHKHE-3 gave a hydrolysis half-life of 2.5 h at 37 °C compared to 8.7 h at 25 °C (Figure 6B, Table 3) at pH 6.0. The hydrolysis rates were also dependent on the type of ketal structures present. The hydrolysis half-life of pPGHBKHE-1 at pH 4.1 and 5.5 was 3 days and 152 days, respectively, at 37 °C (Figure 6C, Table 3). There was no significant hydrolysis (<5%) observed for pPGHBKHE-1 and pPGCHKHE-1 at pH 7.4, even after 400 days at 37 °C. All these data support the fact that degradation of PKHE polymers can be also modulated by changing the temperature apart from the ketal group structure.

2.3.5. Degradation of pPKHE Polymers Determined by GPC Analysis. Information regarding the molecular weights of degradation products of the polymer and the uniformity of ketal monomer incorporation within the polymers was obtained from GPC analysis. The GPC chromatograms for pPDMKHE-3, pPCHKHE-3, and pPGHBKHE-1 before and after degradation are shown in Figure 7. All the polymers showed a monomodal distribution of chains before hydrolysis with no evidence of low-molecular-weight fractions in the sample. Upon hydrolysis, a shift in the chromatogram towards higher elution volume was observed for all the polymers, indicating that they were completely degraded to low-molecular-weight fragments. Together with ^{13}C NMR data (section 2.2), the GPC data confirmed that the ketal groups are uniformly incorporated in the polymer backbone. Similar results were obtained for the other pPKHE polymers.

2.4. Functionalization and Cellular Uptake of PKHEs.

2.4.1. Functionalization of PKHEs. Polymer functionalization with reactive groups such as azides or amines will facilitate the conjugation of fluorophores or other bioactive molecules to the polymer. In order to incorporate various functionalities in the polymer, initially the hydroxyl groups of pPKHEs were reacted with sodium hydride and α-azido-$(PEG)_8$-ω-epoxide to synthesize azido-functionalized polymers (Figure 3). The azide groups were then reduced with triphenylphosphine/water to generate the amine-functionalized polymers. The ketal groups were found to be stable under the reaction conditions developed. In order to investigate the cellular uptake of pPKHEs, fluorescently labeled polymers (FL-pPKHEs) were prepared by the reaction of the amine-functionalized polymers with Alexa-488 carboxylic acid *N*-hydroxysuccinimidyl ester (Figure 3). The unreacted fluorophore was removed by dialysis of the polymer solutions in phosphate buffer at pH 9. The conjugation of the fluorophore to the polymers was confirmed by fluorescence emission spectra at 515 nm.

2.4.2. Cellular Uptake and Degradation of pPKHEs. Controlled intercellular degradation is an important criterion for the development of drug delivery devices for efficient rapid endosomal escape and cytosolic delivery.[22a] It has been shown that, during endocytosis and endosomal maturation, there is a gradual change in the pH from 6.0−6.2 in early endosome to 5.5 in late endosome to 4.5−5 in lysosome.[33] Thus, developing polymeric systems that can rapidly degrade in a controlled way could possibly disrupt the endosome due to osmotic imbalance and help endosomal escape and cytosolic delivery of therapeutic agents.[34−43] Thus, we investigated the degradation of pPKHE polymers in cells using fluorescent derivatives. The cellular uptake and subsequent trafficking of fluorescent-labeled polymers were examined using confocal microscopy at various time intervals. The CHO cells were incubated with FL-pPKHEs (10 mg/mL) for 1 h at 37 °C and were washed with Dulbecco's phosphate-buffered saline before placing them in fresh media at 37 °C, and the cells were viewed at various time intervals. The uptake of all three polymers, FL-pPDMKHE-3 (rapidly degrading), FL-pPCHKHE-3 (slow degrading), and FL-pPGHBKHE-1 (stable at physiological pH), was observed

dx.doi.org/10.1021/ja305080f | J. Am. Chem. Soc. 2012, 134, 14945−14957

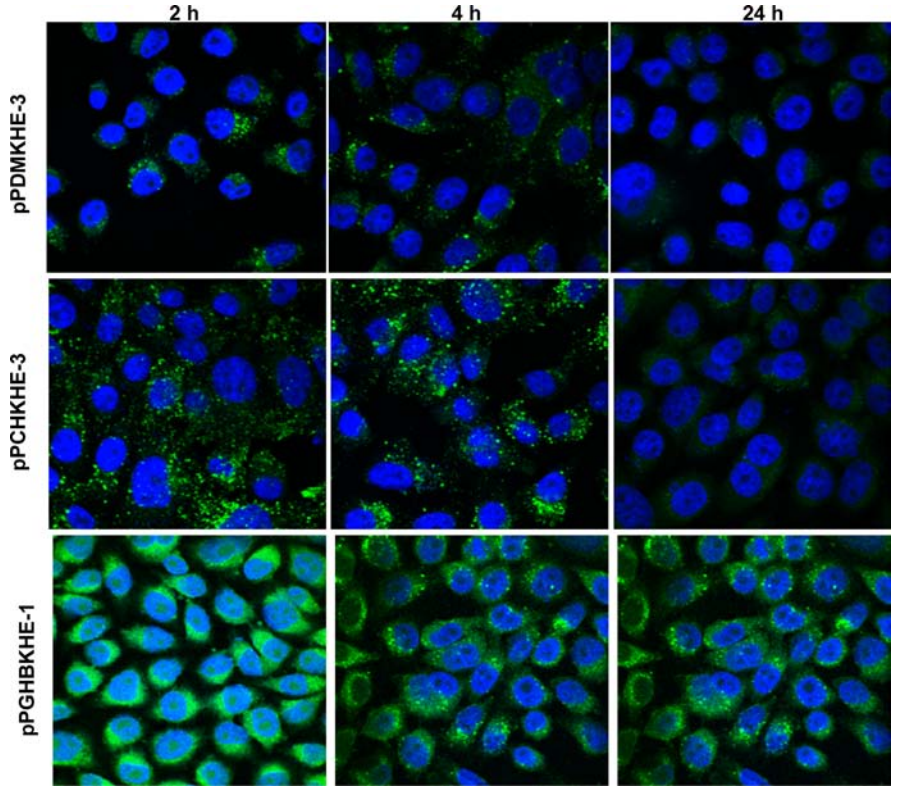

Figure 8. Confocal microscopy images of Chinese hamster ovarian (CHO) cells incubated with fluorophore labeled polymers 2, 4, and 24 h post-treatment. The polymers are labeled with Alexa-488 (green). The nuclei are stained blue using DAPI. Diffused fluorescence observed for pPDMKHE-3 at 4 and 24 h post-treatment and pPCHKHE-3 at 24 h post-treatment suggests degradation of the polymers within the cells and delivery of fluorescent markers into the cytosol. Fluorescence for the slowest degrading polymer pPGHBKHE-1 appeared as distinct points even after 24 h, suggesting that these polymers are still within the various compartments in the cells.

(Figure 8). At 2 h post-incubation, all the polymers were observed as punctate dots, indicating that they are entrapped within the endosomes as reported.[22a,44] At 4 h post-treatment, the rapidly degrading FL-pPDMKHE-3 was visible as diffused green fluorescence and as punctate dots in distinct compartments within the cells (Figures 8 and S25). Both the slowly degrading FL-pPCHKHE-3 and the stable FL-pPGHBKHE-1 polymers presented mostly as punctate dots, indicating that they are still entrapped within the endosomes. At 24 h, the discrete points of the fluorescence were not visible for both FL-pPDMKHE-3 and FL-pPCHKHE-3; instead a diffused intracellular fluorescence was observed, suggesting the degradation of the polymers and release of low-molecular-weight polymer fragments along with fluorescence marker to the cytosol. For the slowest-degrading polymer FL-pPGHBKHE-1, fluorescence was confined to discrete points even 24 h post-incubation, indicating that this polymer was still retained in the endosomes or lysosome without noticeable degradation or excretion from cells.[45] At 4 h post-treatment, the fast-degrading FL-pPDMKHE-3 has the lowest number of punctate fluorescent dots and relatively more diffused fluorescence compared to other polymers. These data together with the results obtained after 24 h suggest that the intracellular degradation of PKHE polymers in the cells may follow a similar trend as observed in the NMR degradation studies in solution (Figures 4–6). The decrease in the number of punctate fluorescent dots and increase in the diffused fluorescence for rapidly degrading pPDMKHE-3 and slowly degrading pPCHKHE-3 in the cells with time may not be due to the exocytosis or the loss of the polymer from cells. This is supported by the fact that the cells treated with equal concentrations of stable pPGHBKHE-1 polymer have considerable amount of punctate fluorescent dots at treatment intervals identical to those of pPDMKHE-3 and pPCHKHE-3 (Figures 8 and S25). The data from pPDMKHE-3 and pPCHKHE-3 also confirmed the delivery of fluorescent molecule (a surrogate drug) into cytosol. Taken together, these results support the fact that the PKHE polymers may have similar degradation profiles in cells as seen in solution, which makes them highly suitable for intercellular drug delivery applications.

2.5. Biocompatibility of PKHEs and Their Degradation Products. Biocompatibility of polymers and their degradation products is critical for their use in various biomedical applications.[46] Therefore, cell and blood compatibilities of the newly synthesized pPKHEs and their degradation products were studied by measuring the cell viability, blood coagulation, complement activation, and platelet activation in their presence.

2.5.1. Cell Viability against Human Umbilical Vein Endothelial Cells. The cell viability of pPKHEs and their degradation products was assessed by incubating human umbilical vein endothelial cells (HUVEC) with increasing polymer concentrations for 48 h and measuring the viable cells by MTS assay. Results are shown in Figure 9A; the polymers showed high cell viability up to a concentration of 5 mg/mL. The degradation products of pPKHEs were also found to be nontoxic to the cells (Figure S26). These results demonstrate the excellent cell compatibility of the new polyketal polymers.

2.5.2. Blood Compatibility. 2.5.2.1. Blood Coagulation. The interaction of polymers with blood components could alter the blood coagulation and may lead to thrombotic

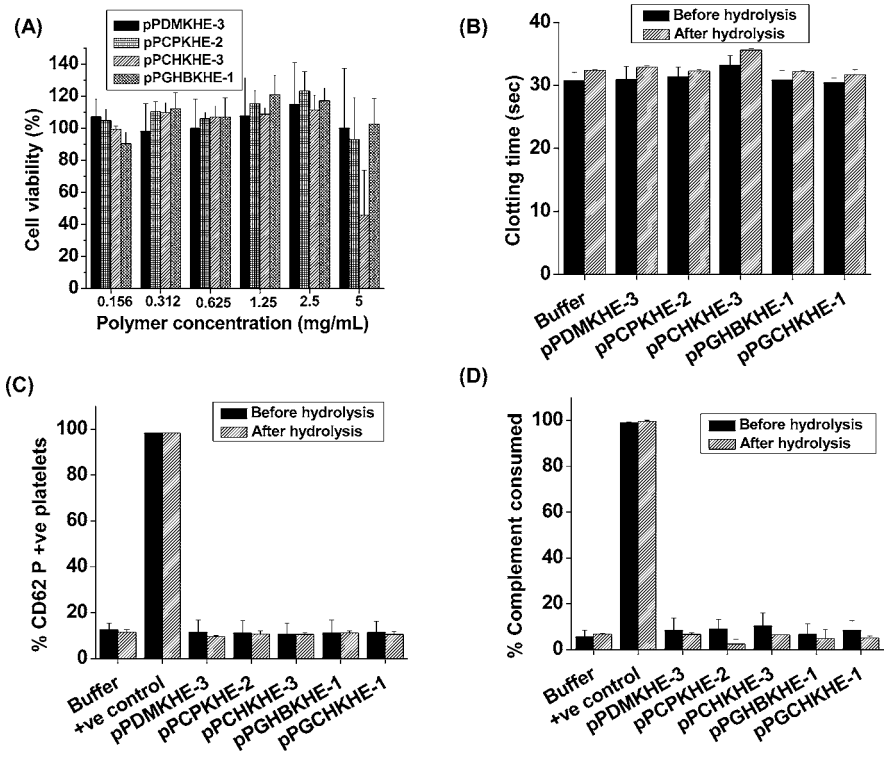

Figure 9. Biocompatibility of pPKHEs and their degradation products. (A) Cell viability of human umbilical vein endothelial cells measured by MTS assay. (B) Activated partial thromboplastin time (APTT) in human plasma measured at 37 °C. HEPES buffer was used as normal control. (C) Platelet activation in human platelet-rich plasma by measuring the expression of activation marker CD62P as measured by flow cytometry. Bovine thrombin and HEPES buffer were used as positive and normal controls, respectively. (D) Complement activation in human serum measured by a complement consumption assay (CH50) using antibody-sensitized sheep red blood cells. The percentage of complement proteins consumed is given. All the blood compatibility tests were performed at a polymer concentration of 1 mg/mL. The data given are from triplicate measurements using three different donors.

complications upon intravenous administration.[46] Such information is critical for the development of drug delivery vehicles for intravenous applications. So the blood coagulation in the presence of pPKHEs and their degradation products was studied by measuring the blood clotting time using clinical coagulation assays.[47] The polymer solutions (1 mg/mL) were incubated with human platelet-poor plasma (PPP) at 37 °C, and the clotting time was measured by activated partial thromboplastin time (APTT), which represents the intrinsic pathway of blood coagulation. APTT is the time (in seconds) taken for a fibrin clot to form after the addition of partial thromboplastin reagent (actin) and calcium chloride. As shown in Figure 9B, pPKHEs and their degradation products did not show significant change in the APTT values compared to that of the buffer control, which indicated that these polymers may not cause any adverse effect on blood coagulation.

2.5.2.2. Platelet Activation. Platelet activation on interaction with polymers can also lead to several adverse effects, such as thrombotic complications and arterial embolization.[46a] Platelet activation results in the expression of the glycoprotein P-selectin CD62 on the surface of platelets, and this was measured by flow cytometry analysis. Polymer solutions (1 mg/mL, final concentration) were incubated with platelet-rich plasma (PRP) for 30 min, and the platelet activation was measured from the expression of platelet activation marker CD62P using monoclonal anti-CD62P-FITC antibody. Platelet activation by pPKHEs was compared with that of buffer control and a positive control (thrombin) and is expressed as the percentage of platelets that are positive for CD62P. The extent of platelet activation by the PKHE polymers and their degradation products was very similar to that of the buffer control (Figure 9C), indicating that the new polymers did not induce any platelet activation.

2.5.2.3. Complement Activation. The complement system consists of a series of proteins circulating in the blood as precursors and is part of the innate immune system. Activation of the components of the complement system upon interaction with a foreign material can produce anaphylotoxins, which can result in cellular responses such as histamine release and induction of inflammation.[46a] It has been shown that hydroxyl-carrying polymers such as starch, poly(vinyl alcohol), and dextran can activate the complement system.[48] However, hydroxyl-containing polymers such as hyperbranched polyglycerol[49] and some glycopolymers[50] did not induce complement activation. To investigate whether the new PKHE polymers activate the complement system, the level of complement activation by pPKHE polymer was studied by antibody-sensitized sheep erythrocyte complement lysis (CH50) assay that measures the total complement activity from the ability of the serum sample to lyse sheep red blood cells coated with IgM antibody.[51] The polymer samples were incubated at 37 °C for 1 h with human serum to which the antibody-sensitized sheep erythrocytes were added. Lysis of the sheep erythrocytes indicative of unactivated complement and the RBC lysis were quantified by measuring the amount of hemoglobin released. Thus, the total amount of complement consumption by the polymer was measured and compared with positive control (immunoglobulin G, IgG), negative control

dx.doi.org/10.1021/ja305080f | J. Am. Chem. Soc. 2012, 134, 14945−14957

(EDTA-incubated serum), and a buffer control. Results shown in Figure 9D confirm that the new polyketal polymers do not activate the complement system.

3. CONCLUSIONS

We reported a new series of well-defined, neutral, highly biocompatible, dendritic multifunctional main-chain degradable hydroxyl-carrying polyether polymers containing structurally different ketal linkages and defined degradability. The polymers were prepared by the ROMBP of α-epoxy-ω-hydroxyl-functionalized ketal monomers. The degradation of polyether polyketals depended on the temperature, pH, and the molecular structure of the ketal linkages. The pH-dependent polymer degradation in aqueous acidic solutions was finely tuned by changing the bonding structure at the ketal linkages; both cyclic and linear ketal structures were studied. Based on the log *P* values of the monomers and the hydrophobicity measurement of the polymers using pyrene fluorescence, we established that the ketal structure-dependent degradability of the polymers in solution was mainly due to the differences in the torsional strain associated with the substituted ketal groups. In the case of polymers with acyclic ketal groups, the influence of hydrophobicity on the degradation kinetics cannot be ruled out. A range of hydrolysis rates, from a few minutes to a few hundred days, depending on the polymer structure was achieved at mild acidic conditions. We have shown that the polymer degradation within cells followed a similar pattern to that of the degradation in aqueous solutions and also the delivery of a fluorescent marker into cytosol. We demonstrated that the new multifunctional PKHEs were highly biocompatible from the cell viability and blood compatibility analyses. The new polymers did not change blood coagulation time and did not activate platelets and complement system. The multifunctional nature along with water solubility and excellent biocompatibility make this new class of biodegradable polymers promising candidates for a variety of biomedical applications, including the development of nanodevices for intercellular drug delivery.

■ ASSOCIATED CONTENT

Ⓢ Supporting Information

Experimental details and additional characterization (^{1}H and ^{13}C NMR, IR, and GPC of the monomer and polymers), polymer degradation, and cellular uptake data. This material is available free of charge via the Internet http://pubs.acs.org.

■ AUTHOR INFORMATION

Corresponding Author

jay@pathology.ubc.ca

Notes

The authors declare the following competing financial interest(s): R.A.S., J.K.N., K.G.R., M.M., and J.N.K. have filed a PCT application based on this work.

■ ACKNOWLEDGMENTS

This research was funded by Alnylam Pharmaceuticals and Canadian Institutes of Health Research (CIHR). The Macromolecular Hub at the UBC Centre for Blood Research was funded by Canada Foundation for Innovation and Michael Smith Foundation of Health Research (MSFHR). J.N.K. is a recipient of a CIHR/CBS new investigator in Transfusion Science and MSFHR career Investigator Award.

■ REFERENCES

(1) Kim, J.; Lee, J. E.; Lee, S. H.; Yu, J. H.; Lee, J. H.; Park, T. G.; Hyeon, T. *Adv. Mater.* **2008**, *20*, 478.
(2) Blanco, E.; Kessinger, C. W.; Sumer, B. D.; Gao, J. *Biol. Med.* **2008**, *234*, 123.
(3) van Vlerken, L. E.; Amiji, M. M. *Exp. Opin. Drug Deliv.* **2006**, *3*, 205.
(4) Uhrich, K. E.; Cannizzaro, S. M.; Langer, R. S.; Shakesheff, K. M. *Chem. Rev.* **1999**, *99*, 3181.
(5) You, J.; Almeda, D.; Ye, G. J. C.; Auguste, D. T. *J. Biol. Eng.* **2010**, *4*, 15.
(6) (a) Wang, Z.; Chui, W.; Ho, P. C. *Pharm. Res.* **2009**, *26*, 1162. (b) Padilla De Jesus, O. L.; Ihre, H. R.; Gagne, L.; Frechet, J. M. J.; Szoka, F. C., Jr. *Bioconjugate Chem.* **2002**, *13*, 453.
(7) Kumar, N.; Langer, R. S.; Domb, A. J. *Adv. Drug Deliv. Rev.* **2002**, *54*, 889.
(8) (a) Heller, J.; Barr, J. *Biomacromolecules* **2004**, *5*, 1625. (b) Heller, J.; Barr, J.; Ng, S. Y.; Abdellauoi, K. S.; Gurny, R. *Adv. Drug Deliv. Rev.* **2002**, *16*, 1015. (c) Wang, C.; Ge, Q.; Ting, D.; Nguyen, D.; Shen, H.-R.; Chen, J.; Eisen, H. N.; Heller, J.; Langer, R.; Putnam, D. *Nat. Mater.* **2004**, *3*, 190−196.
(9) Heffernan, M. J.; Murthy, N. *Bioconjugate Chem.* **2005**, *16*, 1340.
(10) Paramonov, S. E.; Bachelder, E. M.; Beaudette, T. T.; Standley, S. M.; Lee, C. C.; Dashe, J.; Frechet, J. M. J. *Bioconjugate Chem.* **2008**, *19*, 911.
(11) (a) Ou, M.; Wang, X.; Xu, R.; Chang, C.; Bull, D. A.; Kim, S. W. *Bioconjugate Chem.* **2008**, *19*, 626. (b) Meng, F.; Hennink, W. E.; Zhong, Z. *Biomaterials* **2009**, *30*, 2180.
(12) Zhou, L.; Yu, L.; Ding, M.; Li, J.; Tan., H.; Wang, Z.; Fu, Q. *Macromolecules* **2011**, *44*, 857.
(13) (a) Gillies, E. R.; Jonsson, T. B.; Frechet, J. M. J. *J. Am. Chem. Soc.* **2004**, *126*, 11936. (b) Gillies, E. R.; Goodwin, A. P.; Frechet, J. M. J. *Bioconjugate Chem.* **2004**, *15*, 1254. (c) Jung, J.; Lee, I.; Lee, E.; Park, J.; Jon, S. *Biomacromolecules* **2007**, *8*, 3401.
(14) Wischke, C.; Neffe, A. T.; Steuer, S.; Lendlein, A. *J. Controlled Release* **2009**, *138*, 243.
(15) Nasongkla, N.; Bey, E.; Ren, J.; Ai, H.; Khemtong, C.; Guthi, J. S.; Chin, S.-F.; Sherry, A. D.; Boothman, D. A.; Gao, J. *Nano Lett.* **2006**, *6*, 2427.
(16) (a) Hubbell, J. A.; Thomas, S. N.; Swartz, M. A. *Nature* **2009**, *462*, 449. (b) Duncan, R. *Anti Cancer Drugs* **1992**, *3*, 175.
(17) (a) Stubbs, M.; McSheehy, P. M. J.; Griffiths, J. R.; Bashford, C. L. *Mol. Med. Today* **2000**, 15. (b) Hu, Y.; Litwin, T.; Nagaraja, A. R.; Kwong, B.; Katz, J.; Watson, N.; Irvine, D. J. *Nano Lett.* **2007**, *7*, 3056. (c) Edinger, D.; Wagner, E. *Nanomed. Nanobiotech.* **2011**, *3*, 33. (d) Roux, E.; Francis, M.; Winnik, F. M.; Leroux, J. *Int. J. Pharm.* **2002**, *242*, 25. (e) Ulbrich, K.; Subr, V. *Adv. Drug Deliv. Rev.* **2004**, *56*, 1023.
(18) (a) Lee, S.; Yang, S. C.; Heffernan, M. J.; Taylor, W. R.; Murthy, N. *Bioconjugate Chem.* **2007**, *18*, 4. (b) Yang, S. C.; Bhide, M.; Crispe, I. N.; Pierce, R. H.; Murthy, N. *Bioconjugate Chem.* **2008**, *19*, 1164. (c) Sy, J. C.; Seshadri, G.; Yang, S. C.; Brown, M.; Oh, T.; Dikalov, S.; Murthy, N.; Davis, M. E. *Nat. Mater.* **2008**, *7*, 863. (d) Fiore, V. F.; Lofton, M. C.; Roser-Page, S.; Yang, S. C.; Roman, J.; Murthy, N.; Barker, T. H. *Biomaterials* **2010**, *31*, 810. (e) Heffernan, M. J.; Kasturi, S. P.; Yang, S. C.; Pulendran, B.; Murthy, N. *Biomaterials* **2009**, *30*, 910. (f) Seshadri, G.; Sy, J. C.; Brown, M.; Dikalov, S.; Yang, S. C.; Murthy, N.; Davis, M. E. *Biomaterials* **2010**, *31*, 1372.
(19) (a) Jain, R.; Standley, S. M.; Frechet, J. M. J. *Macromolecules* **2007**, *40*, 452. (b) Bachelder, E. M.; Baudette, T. T.; Broaders, K. E.; Paramonov, S. E.; Dashe, J.; Frechet, J. M. J. *Mol. Pharmaceutics* **2008**, *5*, 876. (c) Cohen, J. L.; Almutairi, A.; Cohen, J. A.; Bernstein, M.; Brody, S. L.; Schuster, D. P.; Frechet, J. M. J. *Bioconjugate Chem.* **2008**, *19*, 876. (d) Broaders, K. E.; Cohen, J. A.; Beaudette, T. T.; Bachelder, E. M.; Frechet, J. M. J. *Proc. Natl. Acad. Sci. U.S.A.* **2009**, *106*, 5497.
(20) Sankaranarayanan, J.; Mahmoud, E. A.; Kim, G.; Morachis, J. M.; Almutairi, A. *ACS Nano* **2010**, *4*, 5930.
(21) (a) Seymour, L. W.; Miyamoto, Y.; Maeda, H.; Brererton, M.; Strohalm, J.; Ulbrich, K.; Duncan, R. *Eur. J. Cancer* **1995**, *31A*, 766.

(b) Kopecek, J.; Kopeckova, P.; Minko, T.; Lu, Z.-R.; Peterson, C. M. *J. Controlled Release* **2001**, *74*, 147.
(22) (a) Kwon, Y. J. *Acc. Chem. Res.* **2012**, *45*, 1077. (b) Li, S. *J. Biomed. Mater. Res.* **1999**, *48*, 342. (c) Holland, S. J.; Jolly, A. M.; Yasin, M.; Tighe, B. J. *Biomaterials* **1987**, *8*, 289. (d) Amass, W.; Amass, A.; Tighe, B. *Polym. Int.* **1998**, *47*, 89. (e) Wu, X. S.; Wang, N. *J. Biomater. Sci. Polymer Edn.* **2001**, *12*, 21.
(23) Oikawa, M.; Wada, A.; Okazaki, F.; Kusumoto, S. *J. Org. Chem.* **1996**, *61*, 4469.
(24) Wohl, R. A. *Synthesis* **1974**, *1*, 38−40.
(25) Dishong, D. M.; Diamond, C. J.; Cinoman, M. I.; Gokel, G. W. *J. Am. Chem. Soc.* **1983**, *105*, 586.
(26) Kayser, M. M.; Clouthier, C. M. *J. Org. Chem.* **2006**, *71*, 8424−8430.
(27) (a) Voit, B. I.; Lederer, A. *Chem. Rev.* **2009**, *109*, 5924. (b) Gao, C.; Yan, D. *Prog. Polym. Sci.* **2004**, *29*, 183. (c) Jikei, M.; Kakimoto, M. *Prog. Polym. Sci.* **2001**, *26*, 1233.
(28) Sunder, A.; Hanselmann, R.; Frey, H.; Mulhaupt, R. *Macromolecules* **1999**, *32*, 4240.
(29) (a) Tetko, I. V.; Gasteiger, J.; Todeschini, R.; Mauri, A.; Livingstone, D.; Ertl, P.; Palyulin, V. A.; Radchenko, E. V.; Zefirov, N. S.; Makarenko, A. S.; Tanchuk, V. Y.; Prokopenko, V. V. *J. Comput. Aid. Mol. Des.* **2005**, *19*, 453. (b) VCCLAB, Virtual Computational Chemistry Laboratory, http://www.vcclab.org, 2005.
(30) (a) Kalyanasundaram, K.; Thomas, J. K. *J. Am. Chem. Soc.* **1977**, *99*, 2039. (b) Kainthan, R. K.; Mugabe, C.; Burt, H. M.; Brooks, D. E. *Biomacromolecules* **2008**, *9*, 886. (c) Wilhelm, M.; Zhao, C.; Wang, Y.; Xu, R.; Winnik, M. A.; Mura, J.; Riess, G.; Croucher, M. D. *Macromolecules* **1991**, *24*, 1033. (d) Maiti, S.; Chatterji, P. R.; Nisha, C. K; Manorama, S. V.; Aswal, V. K.; Goyal, P. S. *J. Colloid Interface Sci.* **2001**, *240*, 630.
(31) Kreevoy, M. M.; Morgan, C. R.; Taft, R. W. *J. Am. Chem. Soc.* **1960**, *82*, 3064.
(32) Deslongchamps, P.; Dory, Y. L.; Li, S. *Tetrahedron* **2000**, *56*, 3533.
(33) (a) Overly, C. C.; Lee, K. D.; Berthaiume, E.; Hollenbeck, P. J. *Proc. Natl. Acad. Sci. U.S.A.* **1995**, *92*, 3156. (b) Murphy, R. F.; Powers, S.; Cantor, C. R. *J. Cell. Biol.* **1984**, *98*, 1757. (c) Kneipp, J.; Kneipp, H.; Wittig, B.; Kneipp, K. *J. Phys. Chem. C* **2010**, *114*, 7421.
(34) Seong, K.; Seo, H.; Ahn, W.; Yoo, D.; Cho, S.; Khang, G.; Lee, D. *J. Controlled Release* **2011**, *152*, 257.
(35) Vasir, J. K.; Labhasetwar, V. *Adv. Drug Deliv. Rev.* **2007**, *59*, 718.
(36) Yessine, M. A.; Leroux, J. C. *Adv. Drug Deliv. Rev.* **2004**, *56*, 999.
(37) Lin, Y. L.; Jiang, G.; Birrell, L. K.; El-Sayed, M, E. *Biomaterials* **2010**, *31*, 7150.
(38) Ho, H. V. B.; Slater, N. K. H.; Chen, R. *Biomaterials* **2011**, *32*, 2953.
(39) Convertine, A. J.; Benoit, D. S. W.; Duvall, C. L.; Hoffman, A. S.; Stayton, P. S. *J. Controlled Release* **2009**, *133*, 221.
(40) Pack, D. W.; Putnam, D.; Langer, R. *Biotech. Bioeng.* **2000**, *67*, 217.
(41) Felber, A. E.; Dufresne, M. H.; Leroux, J. C. *Adv. Drug Deliv. Rev.* **2012**, *64*, 979.
(42) Park, I. K.; Singha, K.; Arote, R. B.; Choi, Y. J.; Kim, W. J.; Cho, C. S. *Macromol. Rapid Commun.* **2010**, *31*, 1122.
(43) Griffiths, P. C.; Nilmini, R.; Carter, M.; Dodds, P.; Murphy, D. M.; Khayat, Z.; Lattanzio, E.; Ferruti, P.; Heenan, R. K.; King, S. M.; Duncan, R. *Macromol. Biosci.* **2010**, *10*, 963.
(44) (a) Douglas, K. L.; Piccirillo, C. A.; Tabrizian, M. *Eur. J. Pharm. Biopharm.* **2008**, *68*, 676. (b) Albertazzi, L.; Serresi, M.; Albanese, A.; Beltram, F. *Mol. Pharmaceutics* **2010**, *7*, 680. (c) Benfer, M.; Kessel, T. *Eur. J. Pharm. Biopharm.* **2012**, *80*, 247. (d) Son, S.; Kim, W. J. *Biomaterials* **2010**, *31*, 133. (e) Bayles, A. R.; Chahal, H. S.; Chahal, D. S.; Goldbeck, C. P.; Cohen, B. E.; Helms, B, A. *Nano Lett.* **2010**, *10*, 4086.
(45) (a) Masedunskas, A.; Porat-Shliom, N.; Weigert, R. *Traffic* **2012**, *13*, 627. (b) Coorsen, J. R.; Schmitt, H.; Almers, W. *EMBO J.* **1996**, *15*, 3787. (c) Reddy, A.; Caler, E. V.; Andrews, N. W. *Cell* **2001**, *106*, 157.
(46) (a) Gobert, M. B.; Sefton, M. V. *Biomaterials* **2004**, *25*, 5681. (b) Hansson, K. M.; Tosatti, S.; Isaksson, J.; Wettero, J.; Texter, M.; Lindahl, T. L. *Biomaterials* **2005**, *26*, 861. (c) Amarnath, L. P.; Srinivas, A.; Ramamurthi, A. *Biomaterials* **2006**, *27*, 1416.
(47) Kainthan, R. K.; Gnanamani, M.; Ganguli, M.; Ghosh, T.; Brooks, D. E.; Maiti, S.; Kizhakkedathu, J. N. *Biomaterials* **2006**, *27*, 5377.
(48) (a) Arima, Y.; Kawagoe, M.; Toda, M.; Iwata, H. *Appl. Mater. Interfaces* **2009**, *10*, 2400. (b) Arima, Y.; Toda, M.; Iwata, H. *Biomaterials* **2008**, *29*, 551. (c) Carreno, M.; Labarre, D.; Jozefowicz, M.; Kazatchkine, M. D. *Mol. Immun.* **1988**, *25*, 165.
(49) (a) Kainthan, R. K.; Janzen, J.; Levin, E.; Devine, D. V.; Brooks, D. E. *Biomacromolecules* **2006**, *7*, 703. (b) Kainthan, R. K.; Hester, S. R.; Levin, E.; Devine, D. V.; Brooks, D. E. *Biomaterials* **2007**, *28*, 4581.
(50) Ahmed, M.; Lai, B. F. L.; Kizhakkedathu, J. N.; Narain, R. *Bioconjugate Chem.* **2012**, *23*, 1050.
(51) Inglis, J. E.; Radziwon, K. A.; Maniero, G. D. *Adv. Physiol. Educ.* **2008**, *32*, 317.